Applied Catalysis B: Environmental 111–112 (2012) 133–140

Contents lists available at SciVerse ScienceDirect

Applied Catalysis B: Environmental

journal homepage: www.elsevier.com/locate/apcatb

Adsorption of thiophene and dibenzothiophene on highly dispersed Cu/ZrO_2 adsorbents

P. Baeza[a,*], G. Aguila[b], G. Vargas[a], J. Ojeda[c], P. Araya[d]

[a] Pontificia Universidad Católica de Valparaíso, Facultad de Ciencias, Instituto de Química, Casilla 4059, Valparaíso, Chile
[b] Universidad de los Andes, Facultad de Ingeniería y Ciencias Aplicadas, Av. San Carlos de Apoquindo 2200, Santiago, Chile
[c] Universidad de Valparaíso, Facultad de Farmacia, Casilla 5001, Valparaíso, Chile
[d] Universidad de Chile, Facultad de Ciencias Físicas y Matemáticas, Departamento de Ingeniería Química y Biotecnología, Casilla 2777, Santiago, Chile

ARTICLE INFO

Article history:
Received 29 April 2011
Received in revised form 6 September 2011
Accepted 20 September 2011
Available online 28 September 2011

Keywords:
Adsorption
Copper
Zirconia
Thiophene
Dibenzothiophene

ABSTRACT

The effect of surface area of copper/zirconia adsorbents on the adsorption of thiophene (T) and dibenzothiophene (DBT) was studied. Adsorbents were prepared with different loads of copper (1–6%), using as support zirconias with different surface areas, obtained by varying the calcination temperature. Lower calcination temperatures allowed obtaining zirconias with higher surface area, but lower crystallinity. The characterization results showed that high surface area zirconias have greater copper dispersion capacity, being the zirconia calcined at the lower temperature, the only able to completely disperse a load of 6% Cu, i.e., Z-300 surface has only highly dispersed copper species, while zirconias with higher calcination temperature have also bulk CuO species. The adsorption capacity of T or DBT on Cu/ZrO_2 increased with copper content, reaching a maximum, which coincides remarkably with the zirconia dispersion capacity. This result indicates that dispersed copper species, in Cu^{1+} state, are responsible for the adsorption of these sulfur organic compounds. Therefore the best adsorption capacities were obtained in adsorbents with high content of such copper species, and these adsorbent can be prepared with high surface area ZrO_2, that is with high dispersion capacity of copper.

1. Introduction

New environmental legislation will require substantial reductions in the sulfur content. In the U.S. Environmental Protection Agency (EPA) sulfur standards will require that the sulfur content in gasoline and diesel fuels is 30 and 15 ppm, respectively [1]. The regulations to reduce the sulfur content in fuels for motor vehicles started in the early 1990s and will be increasingly stringent in the coming decades. The new regulations will require deeper desulfurization when harder to react sulfur species are encountered. Industrially, hydrotreatment (HT) has been used to remove organosulfur compounds from fuels, sulfur reduction will be a high priority for refiners in coming years. The elimination of sulfur is carried out through a process called hydrodesulfurization (HDS). HDS uses $Co–Mo/Al_2O_3$, $Ni–Mo/Al_2O_3$ or $Ni–W/Al_2O_3$ bimetallic catalysts, operated at elevated temperatures (300–400 °C) and pressures (20–100 atm of H_2). Technology based on HDS can adequately desulfurize sulfur compounds such as thiols, sulfides, thiophenes and benzothiophene, but it is unsuccessful in treating dibenzothiophene (DBT) derivatives as they are alkyl derived, for example: 4-methyldibenzothiophene (4-MDBT) and 4,6-dimethyldibenzothiphene (4,6-DMDBT) [2,3].

The new unsupported HDS trimetallic catalyst known as "NEBULA" is used for removal refractory sulfur compounds in "deep desulfurization". It was synthesized by ExxonMobil, Akzo Nobel and Nippon Ketjen, and it is three times better than current Co–Mo HDS catalysts and can produce a diesel with a sulfur content of 10 ppmw [4]. However, the NEBULA catalyst requires greater hydrogen consumption. Another important issue is how organic sulfur is adsorbed on HDS catalysts, in this case the adsorption occurs through the sulfur atom, and depends strongly on the amount and types of substituents, in the organic molecule close to the S atom, there can be strong steric hindrance. Desulfurization by HDS is extremely difficult for the least reactive derivatives of DBT with methyl groups in positions adjacent to S, such as 4-MDBT and 4,6-dimethyldibenzothiophene (DMDBT) [5]. Thus, the use of adsorption to selectively remove sulfur compounds under environmental conditions is an excellent option over HDS.

Several studies have developed this as an alternative or complement to the HDS process and a number of other approaches are being tested, including: oxidative microbial desulfurization [6,7] and oxidative chemical desulfurization [8,9]. Adsorption of thiophene and other organic compounds on different adsorbent types has been investigated for different applications [10–13]. These

* Corresponding author. Tel.: +56 322274930.
E-mail address: patricio.baeza@ucv.cl (P. Baeza).

0926-3373/$ – see front matter © 2011 Elsevier B.V. All rights reserved.
doi:10.1016/j.apcatb.2011.09.026

studies are generally limited to a single adsorbent and/or binary mixtures. To the best of our knowledge, no systematic effort has been made to compare the thiophene adsorption capacity of different types of adsorbents.

The adsorbents remove the thiophenic compounds from commercial fuels via π-complexation, and most of them are published by Yang and collaborators [14–19]. The issue of competitive adsorption in a mixture of different classes of hydrocarbons found in gasoline fractions has not been resolved. π-Complexation adsorption is currently the most promising alternative. Molecular Orbital (MO) calculations and experiments have shown that the refractory compounds (MDBT and DMDBT) bind strongly through π-complexation due to a better electron donation/back-donation ability [14,15]. In the π-complexation mechanism the cations can form the usual σ bonds with their s-orbitals, while their d-orbitals can back-donate electron density to the antibonding π-orbitals of the sulfur rings. The metals that can form strong π-complexation bonding are those that possess empty s-orbitals and available electron density at the d-orbitals necessary for back donation [20], especially the copper Cu(I) electronic configuration $1s^2 2s^2 2p^6 3s^2 3p^6 3d^{10} 4s^0$.

Preliminary studies indicate that samples of Cu supported on zirconia possess significant adsorption capacity of sulfur-containing compounds, at relatively low copper levels. In previous research, copper samples supported on zirconia were studied to separate thiophene from a mixture of 2000 ppmw of thiophene in *n*-octane at room temperature and atmospheric pressure [21]. The results of this work show that the capacity of copper on zirconia to adsorb thiophene increases as the copper content increases and the adsorption capacity depends on the treatment applied to the adsorbent prior to the adsorption test, and the higher capacities are observed in adsorbents treated with a flow of N_2O at 90 °C [22]. It was found that this method generates a higher amount of Cu^{1+} species, which are responsible for the adsorption of sulfur organic compounds [20]. These samples possess notable saturation adsorption capacities of 0.49 mmol of thiophene per gram of adsorbent. The zirconia used as support in this study had a surface area of 36 $m^2\,g^{-1}$ [21], and considering that the results of the study were associated with the dispersion of the Cu^{1+} species, it is of interest to further research the relation between the specific surface area of the support, its dispersion capacity and the adsorption capacity of the adsorbents.

This study presents adsorption experiments aimed at reducing sulfur content in liquid hydrocarbons. We present results of promising sulfur adsorbents of copper supported on zirconia, and the adsorption capacity of these materials to remove thiophene (T) and dibenzothiphene (DBT) from a mixture of thiophene or dibenzothiophene in *n*-octane (2000 ppmw) under ambient conditions, considering the effect of the specific surface area of the support on the adsorption capacity of the organic sulfate compounds.

2. Materials and methods

2.1. Adsorbent preparation

The adsorbents were prepared by dry impregnation of zirconium oxide with aqueous solutions of copper nitrate (Merck p.a.) containing the required amount of salt to render copper concentrations of 1%, 2%, 3%, 4% and 6%. Zirconium oxide was obtained by calcination of commercial zirconium hydroxide (FZO922 MEL Chemicals Inc., USA) at different temperatures: 300, 500 and 700 °C, for 3 h in a muffle furnace. After impregnation of the supports, the adsorbents were dried at 105 °C for 12 h, and then calcined at the same temperature at which the zirconium oxide was calcined, for 3 h in a muffle furnace.

2.2. Adsorbent characterization

The zirconium oxides and the Cu/ZrO_2 adsorbents were characterized by physical adsorption of N_2 in Micromeritics ASAP 2010 equipment, after degasifying the samples at 200 °C for approximately 1 h.

The crystal structure of the zirconium oxides and different adsorbents was determined on a Siemens D-5000 diffractometer using Cu Kα radiation, with a step of 0.02° and a step time of 3 s.

The adsorbent samples were studied by temperature programmed reduction (TPR) experiments in 5% H_2/Ar stream, in order to determinate the different copper oxide species over the zirconia surface. In these experiments, 0.2 g of catalyst was loaded in a quartz reactor and oxidized in situ in a 20 $cm^3\,min^{-1}$ stream of pure O_2 at 300 °C for 1 h. The reactor was cooled to room temperature, was purged for 30 min with pure He, the reducing mixture was introduced at 20 $cm^3\,min^{-1}$, and heating started using a 10 °C min^{-1} temperature rate. The H_2 consumption was determined using a thermal conductivity cell.

The fraction of zirconia surface covered by copper in different Cu/ZrO_2 adsorbents was estimated using the electrophoretic migration technique in Zeta Meter Inc. equipment, model 3.0, fitted with an automatic sample transfer unit. In each measurement, 30 mg of sample were suspended in 300 mL of solution 10^{-3} M of KCl, adjusting the pH with solutions of KOH or HCl 0.1 M, as required, obtaining the isoelectric point of copper oxide and zirconium oxide, and the corresponding point of zero charge of each adsorbent. The sample was used directly after calcination, so was expected to be in an oxidized state.

2.3. Adsorption experiments

Adsorption experiments were performed in a vertical Pyrex reactor equipped with a supporting glass porous disk. A bed of 500 milligrams of different adsorbents was placed in the reactor and oxidized in situ at 300 °C for 1 h under a 20 mL min^{-1} flow of pure O_2. After oxidation, the reactor was cooled down to room temperature and purged with pure He for 30 min. Then, a treatment was used to generate Cu^{1+} species over the zirconia surface [21]. This treatment consisted in reducing the oxidized sample entirely, treating it at 300 °C for 1 h under a 20 mL min^{-1} flow of a 5% H_2/He mixture, cooling down to 90 °C, partially reoxidizing with a 20 mL min^{-1} flow of pure N_2O for 30 min, and cooling down to room temperature.

For the adsorption experiments, the liquid flow was driven into the reactor by means of a peristaltic variable flow mini-pump. The experiment was performed using a mixture of 2000 ppmw of thiophene or dibenzothiophene in *n*-octane (C_8H_{18}) at a feed rate of 0.5 mL min^{-1}. Samples were collected every 5 min, until saturation was achieved; the total time depended on the amount of adsorbent (500 mg) and its adsorption capacity.

The samples were analyzed by gas chromatography using a Perkin-Elmer Autosystem XL equipped with an HP-5 capillary column (*L* 30 m, I.D. 0.53 mm, Film 0.88 μm) and the following conditions: detector at 300 °C, injector at 275 °C, and carrier flow, 15 mL min^{-1} (He). The column temperature was set to increase from 40 °C to 200 °C at a rate of 15 °C min^{-1}. 0.5 μL of the sample volume was injected for each GC-FID run. The limit detection was 2 ppm.

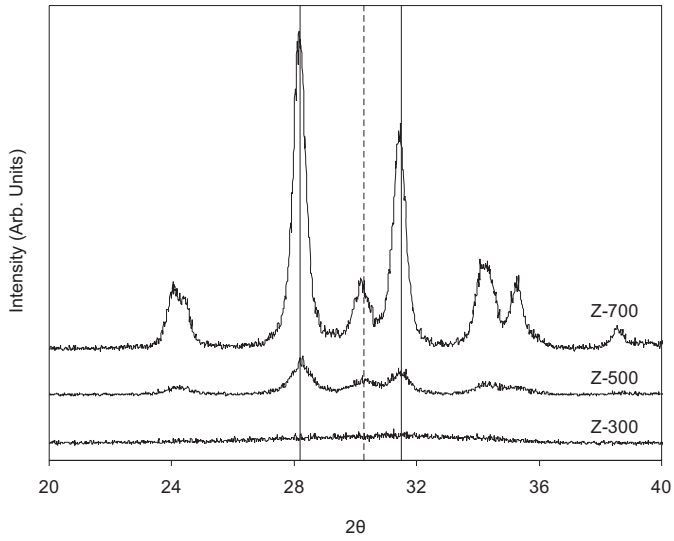

Fig. 1. XRD results of the zirconias calcined at different temperatures. The characteristic diffraction lines of the monoclinic phase (continuous lines) and the tetragonal phase (dotted line) are also included.

3. Results and discussion

3.1. Characterization of supports

3.1.1. Specific area BET

Table 1 shows the specific area BET, microspore volume and pore volume results for the zirconium oxides with different calcination temperatures. It also includes the result of the commercial zirconium hydroxide without calcination, for the purposes of comparison. It can be seen that a decrease in the calcination temperature produces an increase in the specific area and pore volume, but a decrease in the micropore volume of the zirconia. The zirconia calcined at 300 °C (Z-300) shows that the highest specific area (293 $m^2 g^{-1}$), approximately four times the area of the zirconia calcined at 500 °C (Z-500, 70 $m^2 g^{-1}$) and eight times the zirconia calcined at 700 °C (Z-700, 36 $m^2 g^{-1}$).

3.1.2. X-ray diffraction

Fig. 1 shows the XRD results of the zirconias calcined at different temperatures, and the characteristic diffraction lines of the monoclinic phase (28.2° and 31.7°) and the tetragonal phase (30.5°). Similar to the results reported in a previous work [23], the diffractogram of sample Z-700 shows peaks associated with diffraction lines characteristic of both monoclinic and tetragonal phases, included in Fig. 1, with the monoclinic phase showing greater proportion (around 83% [23]). This result can also be seen for sample Z-500, where the diffraction peaks of the monoclinic phase are of higher intensity than the peaks of the tetragonal phase. However, the diffraction peaks of Z-500 are less intense and defined than the diffraction peaks of Z-700, which means that the Z-500 support is less crystalline than Z-700. Therefore, the decrease in calcination temperature leads to a reduction in the crystallinity, along with an increase in specific area of ZrO_2. The latter can clearly be seen in sample Z-300, which with the lowest calcination temperature is precisely the sample with the lowest crystallinity (no diffraction peaks was observed), and at the same time it is the sample with the highest surface area.

3.1.3. Electrophoretic migration

The measurement results for the zeta potential of the supports are shown in Table 2. It can be seen that the isoelectric point of the support decreases along with reduce in calcination temperature. This result is due to a decrease in the number of surface hydroxyl groups as the calcination temperature increases, and also to the decrease in the density of surface acid sites, which is in turn due to the decrease in the surface area of the supports [24].

3.2. Adsorbent characterization

3.2.1. Specific area BET

Considering that the adsorbents are calcined at the same temperature at which the zirconia was calcined, the supports undergo a second calcination at the same temperature for 3 h. It was found that there is a slight decrease in specific area for all adsorbents, and that is independent of the copper load on the support. Table 1 includes the results for adsorbents of 1, 3 and 6% Cu on Z-700, Z-500 and Z-300. The decrease in specific area is on average approximately 10% for any calcination temperature and copper load used in this study. The pore volume increases when the calcination temperature decreases, and does not change with the addition of Cu. The microporosity of the adsorbents studied increases with calcination temperature, probably because it increases the crystallinity of the zirconia support, and does not change with copper content.

3.2.2. X-ray diffraction

The results of XRD experiments of the Cu/ZrO_2 adsorbents showed that the intensity of the peaks of zirconia supports remains unchanged with copper content, and only a very small shift to the right occurs when the diffraction signal associated with crystalline CuO appears. The appearance of these crystalline CuO diffraction peaks depends on the copper content and specific surface area of the zirconia. It should be noted that in this case of Cu/ZrO_2 system there is overlapping of the copper characteristic diffraction peaks (35.5° and 38.7°) with those of the monoclinic zirconia (35.3° and 38.5°), which can somewhat hinder the assignment of crystalline CuO species. For this reason, comparison was made with respect to the base signal of the zirconia, meaning that the increase in peak intensity near to 35.5° and 38.7° may be assigned to the presence of crystalline CuO in the adsorbent. At low copper content is not observed an increase in peak intensity associated with crystalline CuO, indicating that the copper is still quite disperse over the zirconia surface. However, for content of 6% Cu, an increase in peak intensity associated with crystalline CuO can be seen, for both diffraction lines near to 35.5° and 38.7°, but only in the Z-700 and Z-500 supports, as shown in Fig. 2. According to this, the 6% Cu/Z-700 and 6% Cu/Z-500 adsorbents show crystalline CuO species on the support surface. The results obtained on the Cu/Z-700 system are similar to those reported by our research group in a previous study [23], in which a copper load limit (or dispersion capacity) was calculated on Z-700 close to 4% Cu for each 100 $m^2 g^{-1}$ of support. In particular, support Z-700 possesses 36 $m^2 g^{-1}$, and therefore its load limit is close to 1.4% Cu. This means that if the copper load is below 1.4%, only disperse CuO species will be formed, and if the copper load is above this limit any additional amount of copper will form bulk CuO species, which is in agreement with the appearance of crystalline CuO for loads of 6% copper on Z-700. On the contrary, the 6% Cu/Z-300 shows no signal of crystalline CuO. This means that for any copper load used in this study, the CuO species formed on the Z-300 surface are well dispersed and do not form CuO aggregates that may be detected by X-ray diffraction.

Supposing that the zirconia samples with different specific areas are similar in terms of the way that Cu is dispersed (4% Cu for each 100 $m^2 g^{-1}$ of support), it can be estimated that in the case of Z-500, with 70 $m^2 g^{-1}$ specific area, there would a load limit of around 2.8% Cu. This may explain the appearance of crystalline CuO diffraction peak for adsorbent 6% Cu/Z-500, since that this Cu load exceeds the copper dispersion capacity of Z-500 (6% > 2.8%).

Table 1
Specific area BET and microporosity results of zirconias, and Cu supported adsorbents with different calcination temperatures. For comparison, the table includes the characterization of the commercial zirconium hydroxide (MEL Chemicals Inc.) used as precursor.

Sample	Nomenclature	BET Area ($m^2\ g^{-1}$)	Micropore Volume ($cm^3\ g^{-1}\ 10^4$)	Pore Volume ($cm^3\ g^{-1}$)
Commercial $Zr(OH)_4$ (MEL)	ZOH	400	0	0.22
ZrO_2 calcined at 700 °C	Z-700	36	14.5	0.09
1% Cu/Z-700 calcined at 700 °C	1% Cu/Z-700	33	6.81	0.09
3% Cu/Z-700 calcined at 700 °C	3% Cu/Z-700	32	5.63	0.10
6% Cu/Z-700 calcined at 700 °C	6% Cu/Z-700	32	5.05	0.10
ZrO_2 calcined at 500 °C	Z-500	70	4.16	0.16
1% Cu/Z-500 calcined at 500 °C	1% Cu/Z-500	66	0.21	0.15
3% Cu/Z-500 calcined at 500 °C	3% Cu/Z-500	64	0.20	0.15
6% Cu/Z-500 calcined at 500 °C	6% Cu/Z-500	65	0.23	0.14
ZrO_2 calcined at 300 °C	Z-300	293	~0.00	0.24
1% Cu/Z-300 calcined at 300 °C	1% Cu/Z-300	261	~0.00	0.23
3% Cu/Z-300 calcined at 300 °C	3% Cu/Z-300	265	~0.00	0.24
6% Cu/Z-300 calcined at 300 °C	6% Cu/Z-300	263	~0.00	0.24

Table 2
Results of zeta potential measurements: isoelectric point (IEP), potential of zero charge (PZC) and fraction of covered surface (X_M) for the different Cu/ZrO_2 adsorbents.

Sample	Cu load (% w/w)	IEP	PZC	X_M
CuO	–	10.07	–	–
Z-700	–	3.92	–	0.00
1% Cu/Z-700	1.0	–	4.32	0.07
2% Cu/Z-700	2.0	–	5.32	0.23
3% Cu/Z-700	3.0	–	6.94	0.49
4% Cu/Z-700	4.0	–	7.09	0.52
6% Cu/Z-700	6.0	–	7.21	0.54
Z-500	–	3.89	–	0.00
1% Cu/Z-500	1.0	–	3.92	~0.00
2% Cu/Z-500	2.0	–	4.67	0.13
3% Cu/Z-500	3.0	–	5.74	0.30
4% Cu/Z-500	4.0	–	6.43	0.41
6% Cu/Z-500	6.0	–	7.45	0.58
Z-300	–	3.60	–	0.00
1% Cu/Z-300	1.0	–	3.65	0.01
2% Cu/Z-300	2.0	–	4.31	0.11
3% Cu/Z-300	3.0	–	5.17	0.24
4% Cu/Z-300	4.0	–	5.86	0.35
6% Cu/Z-300	6.0	–	6.89	0.51

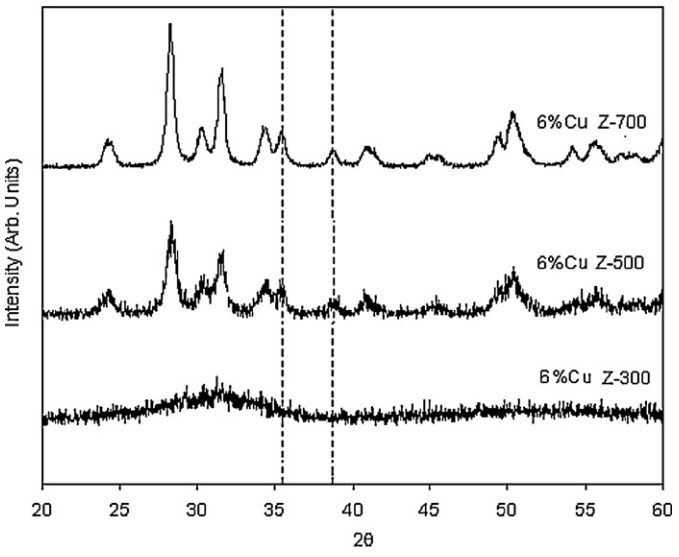

Fig. 2. XRD results for the 6% Cu supported on Z-700, Z-500, and Z-300 adsorbents. The characteristic diffraction lines of CuO (dotted lines) are also included.

Analogously, the copper species formed over Z-300 are only disperse and, within the range of studied Cu loads, no crystalline CuO species or agglomerates are formed that would be detectable by XRD. The reason for this may be the greater surface area available with Z-300 to disperse the copper load. According to the above assumption, given that Z-300 has 293 $m^2\ g^{-1}$ specific area, the load limit would be close to 11.7% Cu. The possibility of studying higher Cu loads on Z-300 is currently in the research stage, and is proposed for future research into load optimization in Cu/ZrO_2 adsorbent systems. Therefore, the formation of different CuO surface species depends directly on the surface area of the zirconia, which in turn depends on calcination temperature.

3.2.3. Temperature programmed reduction by H_2

The results of the temperature programmed reduction experiments of the Cu/Z-700 system are shown in Fig. 3. This system has been studied in previous works [21,23], and the TPR curves and the reduction peaks are particularly well known. In general, peaks with low reduction temperature (170–220 °C) are assigned to disperse CuO species, and peaks of high reduction temperature (270–320 °C) are assigned to bulk CuO species. Remembering that when the copper content over Z-700 (36 $m^2\ g^{-1}$) is less than the load limit (1.4% Cu), the formed CuO species are well dispersed over surface. This is shown in the TPR curve of 1% Cu/Z-700 adsorbent, which shows a reduction peak of copper species at low temperature (with two maximum near to 194 °C and 204 °C). This result fully agrees

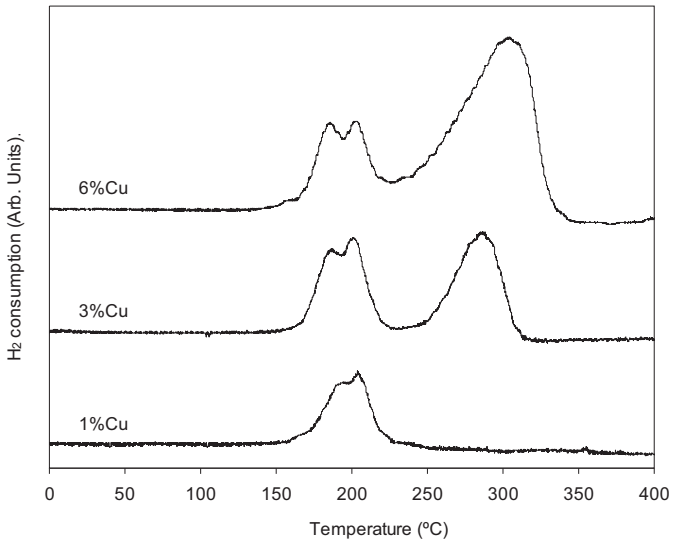

Fig. 3. TPR results for Cu/Z-700 absorbents with different copper loads.

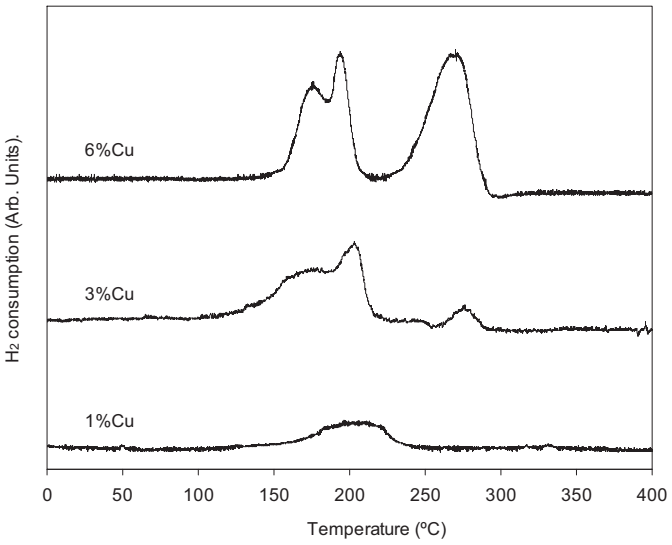

Fig. 4. TPR results for Cu/Z-500 absorbents with different copper loads.

with our previous work [21,23], where it was noted that this peak correspond to the reduction of highly dispersed Cu^{2+} species. The existence of two maximums in this reduction peak was explained considering that these highly dispersed CuO species would be first reduced to Cu^{1+} and then to Cu^0, giving rise to two different maximums (peaks) observed in the TPR curve [25]. Increasing the load to 3% Cu over Z-700, it can be seen that the first peak (peak I) practically maintains its size and position (187 °C and 201 °C), and there also appears a second peak (peak II) of a similar size to peak I (47% and 53%, respectively, by integrating the TPR peaks), but with higher reduction temperature (287 °C). Peak II is assigned to the formation of bulk CuO species on the Z-700 surface, as the copper load on the support is more than double the Cu load limit (3% > 1.4%). Maintaining the above trend, when the load is increased to 6% Cu over Z-700, the proportion of bulk CuO species exceeds that of dispersed CuO species, representing about 74% of the total area of the TPR curve. In this adsorbent, the disperse CuO species maintain their reduction temperature (186 °C and 203 °C), while the bulk CuO species become more difficult to reduce (304 °C), which means an increased state of agglomeration. The increased formation of bulk CuO species in the adsorbents along with the increase in Cu load over Z-700 (3% and 6% Cu) fully coincides with the analysis of the XRD results shown above.

The results of the TPR experiments for Cu/Z-500 adsorbents can be seen in Fig. 4. In the case of 1% Cu/Z-500 adsorbent only one reduction peak can be observed, located close to 204 °C. When the load increases to 3% Cu, a decrease of temperature reduction of copper species was observed, and shows two main peaks: peak I with two maximums (177 °C and 203 °C), and peak II with a maximum close to 276 °C. It is notable that the size of peak II is practically insignificant in comparison to the area of peak I, representing only 9% of the total area. In the case of 6% Cu/Z-500 adsorbent, there are still two peaks: peak I (176 °C and 194 °C), and peak II (269 °C). The increase in Cu load did not lead to a decrease in the reduction temperatures of the formed CuO species. An increase in the size of peak II can also be seen when increasing the load to 6% Cu over Z-500 (54% of the total area), meaning that the added copper mainly formed CuO species with higher reduction temperature (bulk CuO).

Finally, Fig. 5 shows the TPR curves of the adsorbent prepared using Z-300 as support. The 1% Cu/Z-300 adsorbent shows only one peak located at 306 °C. When increasing the copper load to 3%, the peak moves to a lower reduction temperature (282 °C), indicating that the increase in copper content implies both an increase in the area of the TPR peak, that is, higher concentration of surface species of CuO, and also easier reduction of the CuO species. This trend is also seen in the 6% Cu/Z-300 adsorbent, where the reduction peak shows two maximums located at approximately 223 and 234 °C. Recalling the XRD results for the Cu/Z-300 adsorbent, no crystalline CuO was detected at any copper loading, even at the higher load (6% Cu, see Fig. 2). Therefore, it can be said that this copper species are well dispersed over Z-300 surface at any copper load. However, according to the TPR results, these dispersed CuO species have different reducibility, depending on the copper load over Z-300 support.

Some ideas can be taken from the analysis above for the Cu/Z-700 system to explain the systems with Z-500 and Z-300 supports. One case of interest is found with the load of 1% Cu. Considering that this is a low copper load on the supports, it is expected that it will lead to the formation of disperse CuO species only. This is clear for the Z-700 support, whose species show low reduction temperatures. But it is not very notable for the case of 1% Cu/Z-500 adsorbent, as there is a wider peak although with a maximum at a reduction temperature with a range attributable to disperse CuO species (~200 °C). However, 1% Cu/Z-300 adsorbent, whose

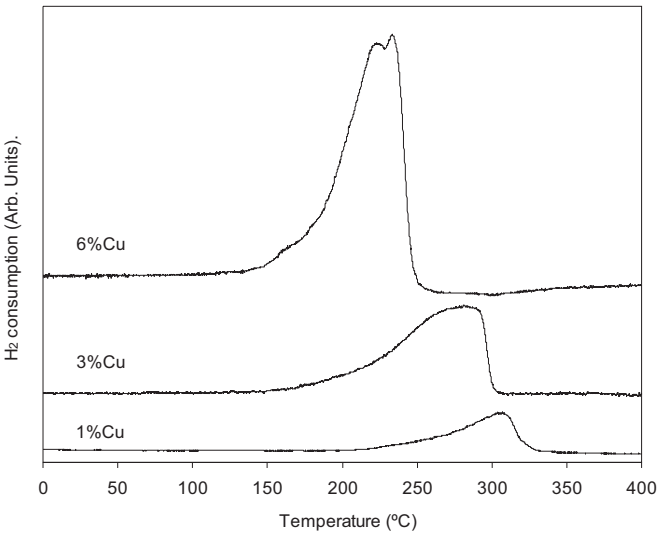

Fig. 5. TPR results for Cu/Z-300 absorbents with different copper loads.

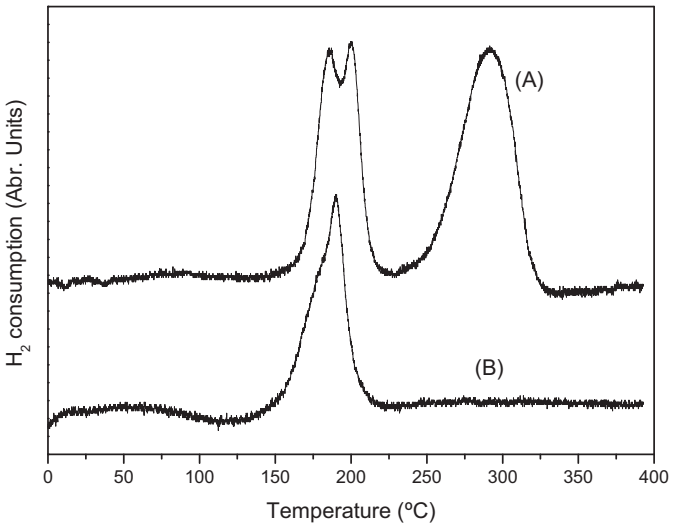

Fig. 6. TPR results for 3% Cu/Z-700 absorbent: (A) oxidized in situ at 300 °C for 1 h; (B) partially reoxidizing with N_2O at 90 °C.

support has a higher surface area, shows a reduction peak at ~300 °C. However, Z-300 is the support with the highest surface area, which gives it greater capacity to disperse the copper. This was shown by XRD result for this adsorbent, where no crystalline (bulk) CuO species was detected. The higher reduction temperature of highly dispersed species of formed CuO on adsorbent 1% Cu/Z-300 is probably due to the strong interaction between the metal and support. This occurrence was also seen in an earlier study [23], and it is not due to the reduction of bulk CuO species.

Recalling the TPR results for adsorbent 3% Cu/Z-500 (Fig. 4), lower presence of bulk CuO species can be seen than in the case of 3% Cu/Z-700 (Fig. 3), since Z-500 support has a greater area, and therefore its load limit is higher (~2.8% Cu). The load of 3% Cu supported in Z-500 slightly passes the load limit, resulting in very low presence of bulk CuO species in comparison with disperse CuO species (9% of relative area). Similarly, 3% Cu/Z-300 adsorbent (Fig. 5) shows only disperse CuO species, since the load limit of Z-300 support have a higher value (close to 11.7% Cu).

Taking into account the existence of a load limit for the supports, it can be said that when the load is 6% Cu, the only support capable of dispersing this amount of copper is Z-300. The proportion of bulk CuO species with regard to the dispersed CuO species is higher when the surface area of the support is lower. Also, it can be said that the disperse CuO species formed in adsorbent 6% Cu/Z-300 shows a higher reduction temperature (~230 °C) than the disperse CuO species on Z-500 and Z-700 (≤200 °C). According to the TPR experiments results, it is probable that the increase in copper load to above 6% using Z-300 as support, the disperse CuO species would have lower reduction temperature, approaching temperatures around 200 °C.

Finally, Fig. 6 compares the TPR curves of 3% Cu/Z-700 absorbent with different pretreatments: (A) oxidized in situ at 300 °C for 1 h, and (B) partially reoxidizing with N_2O at 90 °C. Is clearly seen, that after treatment with N_2O only Cu^{1+} species are observed, which are reduced at lower temperature.

3.2.4. Electrophoretic migration

The results of the zeta potential measurements, isoelectric point (IEP), potential of zero charge values (PZC), and fraction of surface covered by copper oxide (X_M), estimated from the adsorbent PZC, for the different Cu/ZrO_2 adsorbents, are shown in Table 2. It can be seen that the values of the fractions of covered surface for the samples with Z-700 increase with Cu content until reaching a

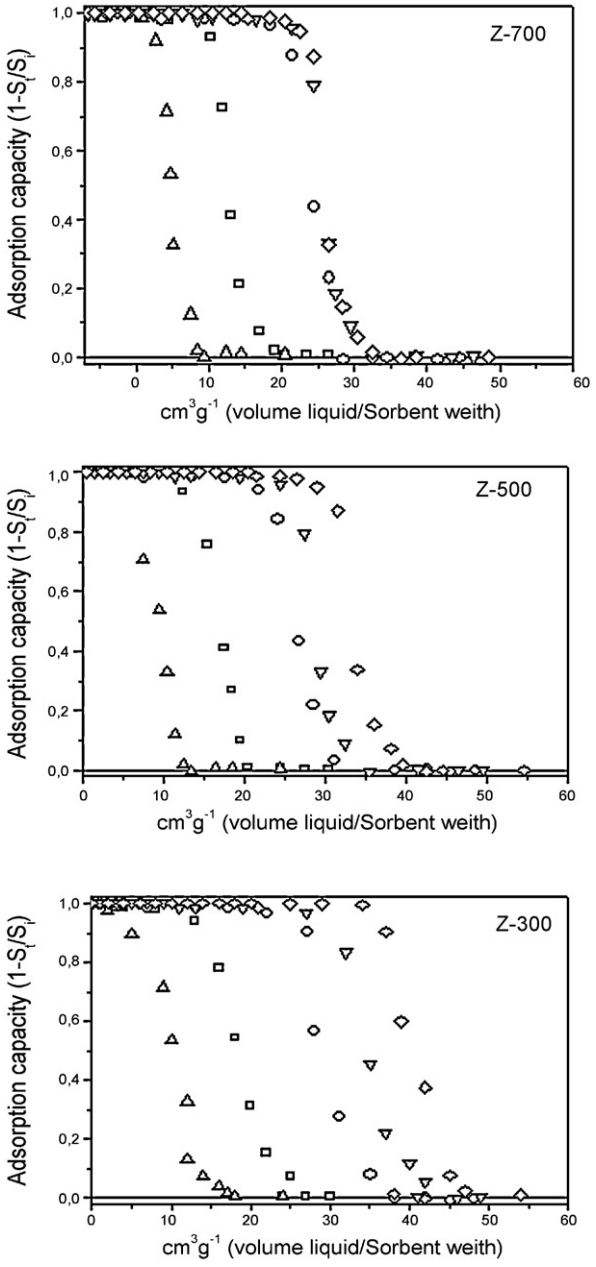

Fig. 7. Adsorption of DBT in bed of Cu/Z-700, Cu/Z-500, and Cu/Z-300, with different copper contents, with a liquid feed containing 2000 ppmw of DBT in *n*-octane. (△) 1% Cu, (□) 2% Cu, (○) 3% Cu, (▽) 4% Cu and (◊) 6% Cu.

maximum at a copper load of 3% (w/w). At higher levels of metal content the surface coverage does not increase, indicating that maximum copper dispersion over Z-700 is reached at loads close to 3% Cu, and above this amount, tridimensional copper species start forming. The difference between the Cu load limit estimated above with XRD and TPR results (1.4% Cu), and the maximum dispersion of copper obtained by zeta potential measurements (~3% Cu) could be explained that in the latter case the bulk CuO species can be considered as species that can cover the surface of Z-700 in the beginning (i.e., at loads not far exceed the copper load limit) along with dispersed CuO species, but at higher copper loads (4% and 6%) bulk CuO species form larger agglomerates that do not contribute in covering the surface, but only in growth over existing CuO species.

The values of the fraction of surface covered for samples with zirconia calcined at 500 °C and 300 °C increase with metal

content, and do not reach a maximum value, as at these calcination temperatures the samples of zirconium oxide that are obtained have larger areas than that obtained with calcination at 700 °C, allowing a larger amount of copper to be loaded onto the surface before bulk copper species begin to form. Therefore, in Z-500 and Z-300 a large amount of disperse copper is obtained on the support surface, which coincides with the results obtained with TPR and XRD experiments. The fraction of covered surface depends directly on the surface area of the support, as is to be expected. On supports with higher surface areas lower fractions of copper covered surface are obtained, but there is a higher amount of disperse copper.

However, it is of note that at high levels of copper content (6%), the fraction of covered surface on all supports is similar and close to 0.5. Recalling that area decreases with temperature, in the sample with the highest area (6% Cu/Z-300), this fraction (0.51) corresponds to a larger amount of square meters covered by copper and therefore the copper (at the same content level) is far more disperse and more available for adsorption of sulfurated organic molecules.

3.3. Adsorption tests

Initial adsorption experiments using Z-700, Z-500, Z-300 and Cu/ZrO_2 samples pretreated with a pure O_2 flow of 20 mL min^{-1} at 300 °C for 1 h (oxidized adsorbent, to obtain Cu^{2+}), or pretreated with a 5% H_2/He flow of 20 mL min^{-1} at 300 °C for 1 h (reduced adsorbent, to obtain Cu^0), show that under these conditions there was no thiophene or dibenzothiophene adsorption. This agrees with results from the literature, which indicate that Cu^{2+} and Cu^0 species do not adsorb thiophene in copper supported on zeolite [20]. Also, this result discards the contribution of the support in the adsorptions capacities of these adsorbents.

To determine the adsorption capacity of the samples, the fraction of adsorbed thiophene or dibenzothiophene was used and the results are expressed as $1 - (S_t/S_i)$, where S_t and S_i are the thiophene or dibenzothiophene concentrations in the outlet and in the initial samples, respectively.

Fig. 7 shows the DBT adsorption curves for the different adsorbents used in this study. Firstly it can be seen that adsorption depends on the copper content present in each adsorbent. This behavior is easily seen at low copper content levels supported on each of the zirconia supports. In addition, it can be seen that adsorption also depends on the calcination temperature of the supports, which is clearly shown at low calcination temperature (Z-300). In this case, the adsorption curve shows a break point at a volume of eluted liquid per gram of adsorbent close to 40 cm^3 g^{-1}, adsorption capacity higher than that of the samples calcined at higher temperatures: 30 and 20 cm^3 g^{-1}, for Z-500 and Z-700, respectively. Another important point, with regard to DBT adsorption by the adsorbents and their dependency on calcination temperature, is the fact that at higher calcination temperature (Z-700) maximum adsorption is reached at copper content close to 3%. On the other hand, for the case of adsorbents prepared with Z-300 and Z-500, a maximum is not reached and adsorption continues increasing along with copper content. This is related to the fact that for the samples prepared with Z-300 (the support with the highest surface area) there is a higher amount of dispersed copper; a result that is in agreement with the sample characterization results obtained using TPR, XRD, and preferentially with the electrophoretic migration results.

Though adsorption of sulfurated molecules by Cu^{1+} species is related to their concentration and dispersion, it should be expected that the samples prepared with Z-300 can be loaded with a larger amount of copper as only 50% of the surface is covered by the metal. An extreme case would be to load copper onto the surface of the precursor zirconium oxide (zirconium hydroxide), which possesses an area of 400 m^2 g^{-1}. In this case the adsorbent sample could not be calcined to obtain CuO over the surface of the zirconia, which is a necessary process for, firstly, transforming the precursor Cu salt into CuO, and secondly, stabilizing the zirconia structure and the CuO on its surface.

By integrating the area under the adsorption curves the saturation adsorption capacities can be estimated, the results of which are shown in Table 3, showing the adsorption capacity of thiophene (T) and dibenzothiophene (DBT) expressed as mmol T or DBT per gram of adsorbent. Firstly, it can be seen that the adsorption of both thiophene and dibenzothiophene depends strongly on the temperature at which the adsorbent was calcined, obtaining higher adsorption capacity for adsorbents prepared with Z-300, that is, on supports with greater surface area that are able to support larger quantities of Cu. Although Z-300 has larger pore volume, the addition of copper causes an increase in the adsorption capacity without producing a change in the pore volume, so the adsorption capacities of the materials is not related to their pore volume and microporosity, but rather the ability to disperse Cu^{1+} species.

The copper in this case is only in the form of dispersed CuO species over the surface and the copper covers a greater area. It can also be seen that the adsorption capacity of adsorbents prepared with Z-700 (36 m^2 g^{-1}) reach a maximum at a copper content level close to 3%, this corroborates the hypothesis that adsorption capacity in this type of system depends on the amount of dispersed CuO. Though the method used to obtain the Cu^{1+} species produces the reduction of all the Cu species (disperse and bulk) prior to treatment with N_2O, it is important to consider that only the well dispersed species are in contact with the sulfurated compound to be adsorbed, and not those that are within the bulk CuO.

Table 3 also shows that the capacities of all adsorbents, whether with high or low amounts of dispersed CuO, are higher for the case in which T is adsorbed than when DBT is adsorbed. This was as expected due to the difference in size between the two molecules. It is, however, notable that although the size of the DBT molecule is more than twice that of the T molecule, the adsorption capacities of DBT are more than half the adsorption capacities obtained for T. For example, for adsorbent 6% Cu/Z-300 the adsorption capacity of thiophene is 0.70 mmol g^{-1} of adsorbent, and for dibenzothiophene it is 0.55 mmol g^{-1}, and while this is obviously a lower adsorption capacity due to the molecule size, one would expect, based on this factor, that the adsorption capacity of DBT would be at least 0.35 mmol g^{-1}. This higher-than-expected adsorption capacity can be explained by the fact that the DBT molecule is more labile to adsorption, as it possesses a higher number of electrons capable of achieving electron retrodonation with the Cu^{1+} species, in comparison with thiophene. As expected, at the same amount of copper on a support with higher area, there is a less amount of copper in the Z-300 expressed as Cu atoms per nm^2; the most important thing is that there is a higher adsorption capacity per copper atom dispersed. Also, it is observed that the optimum concentration of copper depends on the support, and is near to 1 atom of copper per nm^2 of zirconia with higher adsorption capacity. There is a greater adsorption capacity of highly dispersed copper when these copper species were supported on high surface area zirconia (Z-300), considering a load of 1% Cu. In the case of DBT, the adsorption capacity increased from 0.39 to 0.77 adsorbed DBT molecules per dispersed Cu atom, when the zirconia surface area increased from 36 to 293 m^2 g^{-1}. This behavior is very important in order to obtain an adsorbent with high adsorption capacity using small copper content and low calcination temperature. Moreover, this increased adsorption capacity was obtained in molecules that are more refractory to the HDS process.

While thiophene adsorption capacities are lower than those reported for Cu(I)–Y under the same conditions (2.5 mmol g^{-1}) [14], for Cu/ZrO_2 adsorbents the breaking point is closer to saturation, and the copper load could be increased since in this study we used

Table 3
Saturation adsorption capacities of thiophene (T) and dibenzothiophene (DBT) for the different Cu/ZrO_2 adsorbents.

Adsorbent	Cu load (% w/w)	Cu load (atoms nm^{-2})	Adsorption capacity (mmol T (g of adsorbent)$^{-1}$)	Adsorption capacity (mmol DBT (g of adsorbent)$^{-1}$)
Z-700 support	–	–	N.D.	N.D.
1% Cu/Z-700	1.0	2.6	0.22	0.06
2% Cu/Z-700	2.0	5.3	0.32	0.17
3% Cu/Z-700	3.0	7.9	0.49	0.32
4% Cu/Z-700	4.0	10.5	0.49	0.34
6% Cu/Z-700	6.0	15.8	0.49	0.35
Z-500 support	–	–	N.D.	N.D.
1% Cu/Z-500	1.0	1.4	0.26	0.09
2% Cu/Z-500	2.0	2.7	0.37	0.17
3% Cu/Z-500	3.0	4.1	0.52	0.34
4% Cu/Z-500	4.0	5.4	0.54	0.37
6% Cu/Z-500	6.0	8.1	0.59	0.45
Z-300 support	–	–	N.D.	N.D.
1% Cu/Z-300	1.0	0.3	0.27	0.12
2% Cu/Z-300	2.0	0.6	0.39	0.24
3% Cu/Z-300	3.0	0.9	0.54	0.40
4% Cu/Z-300	4.0	1.3	0.61	0.46
6% Cu/Z-300	6.0	1.9	0.70	0.55

N.D., not detected.

lower copper content (6%) than those reported (~23%), indicating a higher efficiency of adsorption per copper atom.

The results shown demonstrate that Cu supported on zirconia is prominent adsorbent in the desulfurization of sulfur organic compounds, with possible applications in deep desulfurization. The adsorption capacity of this Cu/ZrO_2 system is substantially increased by increasing the surface area of the zirconia through use of a lower calcination temperature.

4. Conclusions

The dispersion of copper over samples of zirconia with different surface areas is an important issue in the adsorption capacity of both thiophene and dibenzothiophene by the adsorbent. The surface area depends in turn on the temperature at which the support was calcined. The zirconia loses surface area with an increase in calcination temperature, and also changes its structural conditions, becoming more crystalline.

For high levels of copper load (~4–6%) the order of adsorption capacity is: Z-300 > Z-500 > Z-700. It is important to note that the main factor for adsorption is the existence of disperse CuO species over the support, and other factors such as the crystalline structure of the support, or the reducibility of dispersed copper species have low influence. This result for adsorption capacity is directly related to the Cu load limit of each support, since considering the higher copper load of 6%, the amount of disperse CuO species on the supports Z-300, Z-500, and Z-700 would be 6%, 2.8% and 1.4%, respectively.

Higher than expected adsorption capacities were observed for DBT, even when considering its bigger size, reaching a level of 0.55 mmol adsorbed per gram of adsorbent. This is very promising as the adsorption of this type of molecule (refractory to the HDS process) shows that this type of treatment is efficient and complementary to the traditional HDS process, implying that it could be used to eliminate refractory molecules from petroleum, thus achieving deeper desulfurization.

Acknowledgments

This work has been financed under FONDECYT project 11100165, and FAI Iniciación ICI-001-10 of Universidad de los Andes. Donation of hydrous zirconium by Magnesium Elektron Inc. MEL (USA) is gratefully acknowledged.

References

[1] A. Avidan, B. Klein, R. Ragsdale, Hydrocarbon Process. 80 (2001) 47–53.
[2] B.C. Gates, J.R. Katzer, G.C.A. Schuit, Chemistry of Catalytic Processes, McGraw Hill, New York, 1979.
[3] A. Avidan, M. Cullen, National Petroleum & Refiners Assoc. Annual Meeting. Washington, D.C., March 2001; Paper AM-01-55.
[4] Y. Gochi, C. Ornelas, F. Paraguay, S. Fuentes, L. Alvarez, J.L. Rico, G. Alonso-Núñez, Catal. Today 107 (2005) 531–536.
[5] V. Mille, E. Schulz, M. Lemaire, M. Vrinat, J. Catal. 170 (1997) 29–36.
[6] M. Grossman, in: M.L. Occelli, R. Chianelli (Eds.), Hydrotreating Technology for Pollution Control, Marcel Dekker Inc., New York, 1996, pp. 345.
[7] M. Ayala, R. Tinoco, V. Hernandez, P. Bremauntz, R. Vazquez-Duhalt, Fuel Process. Technol. 57 (1998) 101–111.
[8] Y. Hangun, L. Alexandrova, S. Khetan, C. Horwitz, A. Cugini, D. Link, B. Howard, T.J. Collins, Pet. Chem. Div. Prepr. 47 (2002) 42–44.
[9] V. Hulea, F. Fajula, J. Bousquet, J. Catal. 198 (2001) 179–186.
[10] D.M. Ruthven, B.K. Kaul, Ind. Eng. Chem. Res. 32 (1993) 2053–2057.
[11] J. Weitkamp, M. Schwartz, S. Ernst, J. Chem. Soc., Chem. Commun. 113 (1991) 3–1134.
[12] W.W.C. Quigley, H.D. Yamamoto, P.A. Aegerter, G.J. Simpson, M.E. Bussell, Langmuir 12 (1996) 1500–1510.
[13] J. Yun, D. Choi, S. Kim, AIChE J. 44 (1998) 1344–1350.
[14] A.J. Hernández-Maldonado, R.T. Yang, Ind. Eng. Chem.Res. 42 (2003) 123–129.
[15] A.J. Hernández-Maldonado, R.T. Yang, AIChE J. 50 (2004) 791–801.
[16] A.J. Hernández-Maldonado, S.D. Stamatis, R.T. Yang, A.Z. He, W. Cannella, Ind. Eng. Chem. Res. 43 (2004) 769–776.
[17] R.T. Yang, Adsorbents: Fundamentals and Applications, Wiley, New York, 2003.
[18] R.T. Yang, A. Takahashi, F.H. Yang, Ind. Eng. Chem. Res. 40 (2001) 6236–6239.
[19] R.T. Yang, A.J. Hernández-Maldonado, F.H. Yang, Science 301 (2003) 79–81.
[20] A.J. Hernández-Maldonado, R.T. Yang, Catal. Rev. 46 (2004) 111–150.
[21] P. Baeza, G. Aguila, F. Gracia, P. Araya, Catal. Commun. 9 (2008) 751–755.
[22] A. Dandekar, M.A. Vannice, J. Catal. 178 (1998) 621–639.
[23] G. Aguila, S. Guerrero, F. Gracia, P. Araya, Appl. Catal. A 305 (2006) 219–232.
[24] F.J. Gil-Lambías, A.M. Escudey-Castro, Chem. Commun. 1 (1982) 478–479.
[25] Z. Liu, M. Amiridis, Y. Chen, J. Phys. Chem. B 109 (2005) 1251–1255.